1st Conference on Nuclear Cross Sections and Technology - Washington 3-7 March 1

J. Lachkar, G. Haouat, M.T. Mc Ellistrem*, Y. Patin, J. Sigaud, J. Coyne
Service de Physique Nucléaire - Centre d'Etudes de Bruyères-le-Châtel
B.P. n° 61 - 92120 Montrouge, France.

Differential cross sections for neutron elastic and inelastic scattering from ^{76}Se, ^{78}Se, ^{80}Se and ^{82}Se, have been measured at 8 MeV incident neutron energy and from ^{76}Se and ^{82}Se at 6- and 10 MeV incident energies. The differences observed in the elastic scattering cross sections are interpretable as the effects of isospin term in the scattering potentials. A full analysis of the elastic scattering data are presented.

(Nuclear Reactions $^{76,78,80,82}Se(n,n)$, (n,n'), E=6-10 MeV ; measured σ(θ) ; deduced optical-model parameters ; Enriched targets).

Introduction

In recent years, a large quantity of accurate elastic scattering data for protons in addition to heavy nuclei have been collected. They have been used to deduce various sets of proton nucleus optical - model parameters[1,2]. For neutrons, elastic scattering data are less numerous and accurate than for protons. Also, most of the measurements have been made at low neutron energies where the compound elastic contribution cannot be neglected. In addition to this lack of data, many features of the optical model seem to be still unclear for neutrons, namely the energy and the isospin dependence of the parameters[2]. In order to improve the understanding of neutron-nucleus scattering we have undertaken the study of elastic and inelastic scattering of neutrons from the enriched isotopes ^{76}Se, ^{78}Se, ^{80}Se, ^{82}Se over the neutron energy range 6 to 10 MeV.

There are several reasons why a study of these Se isotopes is of particular interest. Firstly, for the four separated Se isotopes, the isospin dependence of the optical model parameters can be investigated over a relatively large range of the $\frac{N-Z}{A}$ asymetry term (0.165 0.184). Secondly, these isotopes have neutron numbers between 42 and 48, that is just below the closed shell at N = 50. In this mass region, Lane et al.[3] have pointed out that some shell effects may induce a strong decrease in the magnitude of the imaginary part of the optical potential. Finaly, this element is in a region of spherical nuclei where the deformation effects are low and therefore where the optical model gives a good description of the shape elastic scattering.

Experimental procedure

Differential cross section measurements were performed using the neutron time-of-flight facility of the Centre d'Etudes de Bruyères-le-Châtel. The experimental set-up is extensively described elsewhere[4] and therefore only a brief description will be given here.

The $D(d,n)^3He$ reaction measured to produce the incident neutrons at 8-MeV energy and at 6- and 10- MeV energies, the incident neutrons were produced from the $T(p,n)^3He$ reaction. Deuterons or protons were accelerated by the tandem Van de Graaff accelerator. The beam was pulsed and bunched so that 1 ns bursts at a frequency of 2.5 MHz were available. The average beam currents were approximately 3 μA both for deuterons and for protons.

The samples were powders of metallic isotopically enriched Se isotopes, weighing about 50 g each, on loan from Russia. They were contained in polyethylene cans of diameter 25 mm and height 50 mm. The cell-to-sample distance was about 12 cm.

Scattered neutrons were detected independently by four detectors. Each of them was composed of a NE213 liquid scintillator, 12.7 cm in diam by 5 cm thick, mounted on a fast photomultiplier (XP1040). Each detector was housed in heavy shield of polyethylene and lead behind a 1.5 m long collimator of paraffin loaded with lithium and boron. Four 70 cm long iron shadow bars with tungsten tips reduced the background caused by direct neutrons coming from the target. To prevent from gamma events, we employed pulse-shape discrimination. The flight path length was 8 m for the three incident neutron energies. The measurements were made using standard time-of-flight techniques. In the data reduction process, the time-of-flight spectra were sorted off line for neutron-energy thresholds of 1.5 MeV at 6- and 8-MeV neutron energies and of 2.5 MeV at 10- MeV energy.

The energy dependence of the neutron detector efficiency was measured by two independent methods. In the first one, we counted directly monoenergetic neutrons from the target produced by the $D(d,n)^3He$ reaction. In the second one, a (n-p) scattering experiment was performed using a polyethylene sample (1 cm diam. by 4 cm-height).

An auxiliary liquid scintillator with n-γ discrimination was used, with the time-of-flight method, for monitoring the primary neutron beam. The neutron flux was measured with a proton recoil counter telescope, placed at 0°, which had the same solid angle as that of the sample.

The measurements were corrected for finite sample effects using both an analytic method and a monte carlo method ; the corrected values were consistent within 3 per cent. The overall accuracy of the measurements ranged from 5 to 20 %.

Results and discussion

Differential cross sections for neutron elastic and inelastic scattering from ^{76}Se, ^{78}Se, ^{80}Se and ^{82}Se were measured at 8-MeV incident neutron energy and from ^{76}Se and ^{82}Se at 6- and 10- MeV incident energies. Measurements were completed over the angular range from 70 to 150° at 16 to 24 angles in either 5° or 10° steps, with 5° steps taken at the minima of the cross section curves. Incident neutron-energy spreads were between 180 keV at 6- and 10- MeV neutron energies and 300 keV at 8 MeV. They were small enough to ensure good separation at the first excited level but large enough to allow energy-averaged measurements. The elastic scattering data at 6, 8, and 10 MeV are shown in figs.1,2,3 respectively. It is seen that, at each of these energies, the large angle scattering increases with the neutron number of the isotope. On the other hand, the inelastic cross sections to the first 2^+ levels (not shown here) were observed to be exactly the same for ^{76}Se and ^{82}Se at 6- MeV incident energy and very similar for all four isotopes at 8 MeV. The observed likeness of the inelastic scattering to the first excited level in all the isotopes may reflect the fact that the four isotopes have similar deformabilities. Since this effect was observed at 6- and 8- MeV energies, we may assume that channel coupling has a very small contribution to the elastic and inelastic scattering and that the deformation effects are low.

* Present address: University of Kentucky, Lexington, Ky.

The pronounced differences observed in the elastic scattering cross sections are then directly interpretable as the effect of isospin term in the scattering potentials. These effects have been studied, here, by χ^2 fitting of the optical model parameters to the shape elastic angular distributions. For this purpose, we have subtracted from the differential cross sections the compound elastic contribution. This last contribution has been calculated on the basis of the (n,n') reaction studies for selenium isotopes reported elsewhere in these proceedings.

In the analysis of the optical model parameters, we have adopted fixed shapes of the potentials and placed some constraints upon the parameters, the real potential was assumed to be of the Saxon Woods shape, and the imaginary and the spin-orbit potentials are taken to be of the Saxon Woods derivative shapes. Moreover, we have chosen to fix values for the geometrical parameters as follows :

Radii : $R = R_S = R_{1s} = R_o A^{1/3}$ fm. $\quad R_o = 1.25$ fm.

Diffusiveness : $a = a_{1s} = 0.67$ fm.

The adopted value for the radii is that which is the most frequently used[1]. On the other hand, Holmqvist and Wiedling [5] have shown that the real diffusiveness parameter is essentially mass i dependent and equal to 0.66 ± 0.01 fm. With this fixed geometry we avoided some correlated ambiguities, such as the well-known VR^n one (V being the real potential depth).

The imaginary diffuseness a_S was not kept constant. Previous systematic studies of fast neutron elastic scattering have yielded many very different values for a_S ranging from 0.44 to 0.67.

Theoretical considerations predict energy and isospin dependence for both the real and imaginary potentials. The first dependence is a consequence of the non-locality of the nuclear forces[9]. The second is based on the expectation that the optical potential contains an isovector term leading to a dependence on symmetry number $\frac{N-Z}{A}$.[10]

The neutron real and imaginary potentials were assumed to be of the form :

$$V = V_o - \alpha E - \frac{N-Z}{A} V_1$$

$$W_s = W_o - \alpha_S E - \frac{N-Z}{A} W_1$$

where E is the incident laboratory neutron energy $V_o, \alpha, V_1, W_o, \alpha_S$ and W_1 constants to be determined. The spin-orbit potential depth was supposed real and without any dependence.

The optical-model code SPI was used to fit, with search routine, the experimental data. Optimum parameters were obtained by performing series of subsearches on groups of less than six parameters. The main features revealed in the present analysis are as follows :

- The strength of the real potential V_o was determined to an accuracy of less than 1 MeV ; its value : 49.0 is consistent with those obtained for adjacent nuclei and the same value of R[1].

- A linear variation of the real potential with the neutron energy E was assumed. In most cases the α coefficient has been kept fix and equal to the common value of 0.32. When this parameter was let free, good overall fits to the data were obtained for α from 0.25 to 0.34. The value of 0.32 has been adopted.

- The real part of the isospin potential V_1 was found equal to 9.3 ± 1.8 MeV. This value is considerably lower than those obtained by Becchetti and Greenlees[7] (24 MeV), and Dukarevich et al.[7] (17±2 MeV) but consistent within the uncertainties with that reported by Holmqvist and Wiedling[5] (13 ± 6 MeV).

- The completeness of the experimental data mainly at backward angles has allowed an accurate determination of the spin-orbit potential strength. The deduced value, 6.0 ± 1.5 MeV, is very close to that reported by Becchetti and Greenlees[7] (6.2 MeV) although the values of V_{1s} are different in the two sets of optical-model parameters.

- For a_S varying from 0.44 to 0.67 fm, we have deduced the optimized values for W_o and W_1 along with the corresponding χ^2 values. The results are presented in fig. 4. The other parameters have been either kept fix or found nearly constant. The quality of the fit to the data is almost the same for a_S between 0.49 and 0.67 fm. In this range, W_o decreases with a_S so that $W_o.a_S$ is nearly constant. Moreover, in the whole range for a_S, the ratio W_1/W_o remains approximately constant and equal to about 3.2. The deduced values for W_o are in good agreement with those previously reported particularly with that of ref.[7] (W_o=13 MeV with a_S=0.5d fm). The physical meaning of these features will be discussed in the conclusion.

- No evidence for any definite energy dependence of the absorption potential W has been found (α_S=0). The fitting procedures indicated either a constancy of W with E as it was previously proposed by Fesen et al.[11] or a slight increase of W with E qualitatively consistent with that used by Mani et al.[12].

In the adjustment procedures no imaginary volume potential was used at 6 and 8 MeV neutron energies ; good overall fits to the data were obtained for volume absorption potential strength of 0.95 MeV for 10-MeV data.

Conclusion

All the optical-model parameters deduced from this study are consistent with those from previous systematic studies except for one of them, the isospin dependent imaginary potential W_1. In conjunction with an absorption roughly proportional to the product $W_o.a_S$, we have deduced the constancy of the ratio $\frac{W_1}{W_o}$ over a large range for a_S. This constant (3.2) is somewhat anomalously high in comparison to that reported by Becchetti and Greenlees[7] (0.92) or by Dukarevich et al.[7] (1.8). This disagreement may be apparent and due to the neutron numbers of the Se isotopes which are close to the magic number N=50. It may be argued, as it was expected by Lane et al.[3], that W has not only a smooth dependence on N and Z but also a strong decrease near magic numbers. This hypothesis has been previously established by two experiments for the doubly closed shells at A = 40 and A = 208. Holmqvist and Wiedling[5] have reported that the magnitude of W for Ca, found in their study, deviates from the linear dependence of W versus $\frac{(N-Z)}{A}$ as they observed for other elements. On the other hand, Vonach et al.[13] have presented some evidence for a minimum in W near the doubly closed shell at A = 208. We may then conclude that the large deduced value of W_1, inducing a low value of W, reflects the influence of the neutron shell closure at N = 50 on neutron optical-model absorption.

References

1. C.M.Perey and F.G.Perey, Nucl. Data Tables 10 (1972) 539

2. F.D. Becchetti and G.W. Greenlees, Phys. Rev. 182 (1969) 1190

3. A.M. Lane, J.E. Lynn, E. Melkonian and E.R. Rae, Phys. Rev. Lett. 2 (1959) 424

4. G. Haouat, J. Lachkar, J. Sigaud, Y. Patin, F. Coçu, CEA-Report R-4641 (1975)

5. B. Holmqvist and T. Wiedling, Nucl. Phys. A188 (1972) 24

6. D. Wilmore and P.E. Hodgson, Nucl. Phys. 55 (1964) 673

7. Yu. V. Pokarevich, A.N. Bychin and D.H. Fachinter, Nucl. Phys. A92 (1967) 433

8. C.H. Newstead, J. Delaroche, B. Cauvin, Proc. Conf. Int. on Statistical Properties of Nuclei, Albany (1971) 167

9. F.G. Perey and B. Buck, Nucl. Phys. 32 (1962) 353

10. A.M. Lane, Rev. Mod. Phys. 29 (1957) 193 and Nucl. Phys. 35 (1962) 676

11. L. Rosen, J.G. Beery, A.S. Goldhaber and E.H. Auerbach, Ann. Phys. 34 (1965) 96

12. G.S. Mani, M.A. Melkanoff, I. Iori, CEA Report R-2380 (1963)

13. W.G. Vonach, A.B. Smith and P.A. Moldauer, Phys. Lett. 11 (1964) 331

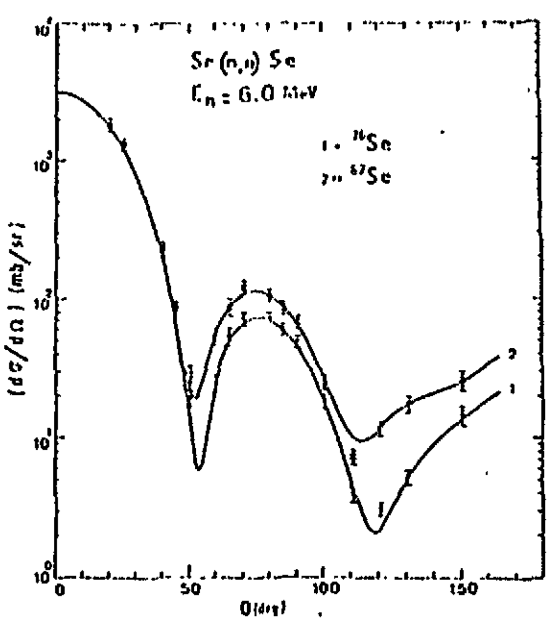

Fig. 1
Elastic scattering angular distributions at 6.0-MeV incident neutron energy for ^{76}Se and ^{82}Se . The solid lines are the results of optical model calculations as described in the text .

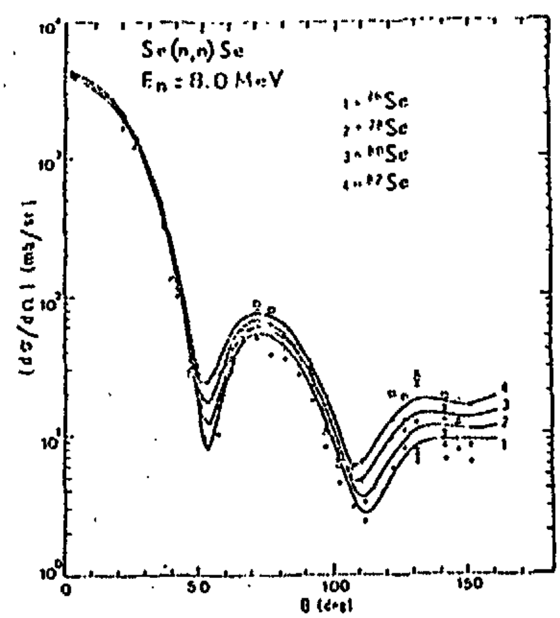

Fig. 2
Elastic scattering angular distributions at 8.0-MeV incident neutron energy for ^{76}Se, ^{78}Se, ^{80}Se and ^{82}Se . The solid lines are the results of optical model calculations as described in the text .

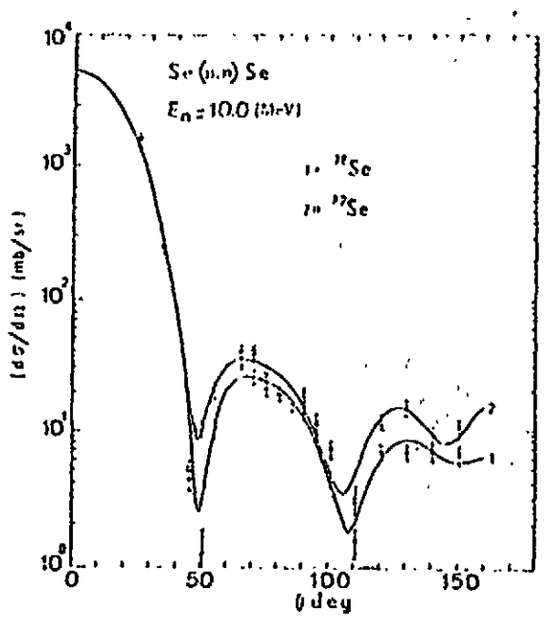

Fig. 3
Elastic scattering angular distributions at 10.0-MeV incident neutron energy for ^{76}Se and ^{77}Se . The solid lines are the results of optical model calculations as described in the text .

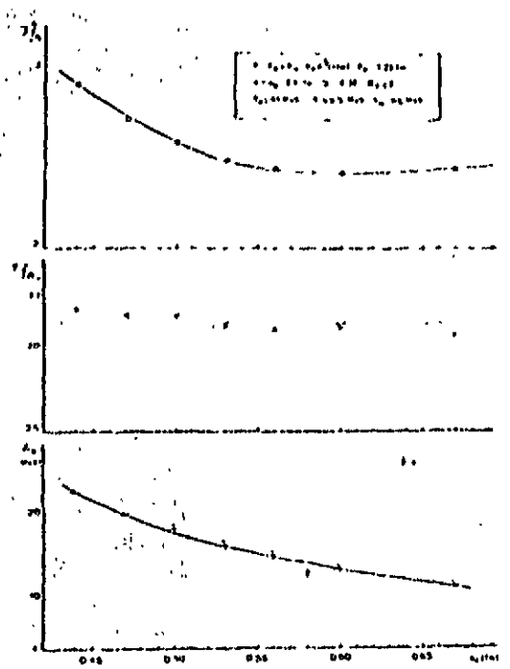

Fig. 4
Variation with the imaginary diffusiveness a_s of the imaginary potential W_0, the ratio W_1/W_0 and the corresponding χ^2/N values .